Simulating Astronomical Images to Determine Crowded Field Photometric Uncertainties
SIRI Final Report

Aaron Bunch

Mentor: Leonidas Moustakas
Co-mentor: Andrew Romero-Wolf

June 2, 2015

Abstract

In support of a pilot project to infer constraints on the dark matter substructure of galaxies by measuring the time delays in two gravitationally lensed quasars, HE0435-1223 and RXJ1131-1231, I developed Python code that uses the GalSim Python library to simulate ground-based images of these objects. The code reads general observational parameters, object parameters, and simulated light curve data, and then generates simulated FITS files of the strongly lensed quasars. When the parameters are finely tuned, the simulated images should be indistinguishable from the real astronomical data, except that the simulated images will have known time delays. The photometric uncertainties can be determined by applying our methods to the simulated images, and comparing our results with the known values.

1 Introduction

The existence of dark matter was hypothesized in the 1930s in order to explain a discrepancy between the observed rotation curve of galaxies and the rotation curve predicted by their visible disk [i]. Given the apparent mass distribution of galaxies, the velocity of stars should diminish with their distance from the galactic center. Instead, we find that velocity levels off or even increases with distance (Figure 1). A roughly spherical halo of dark matter surrounding galaxies, with greater concentration at the center, would account for these observations (Figure 2). It is hypothesized that this dark matter interacts gravitationally with the rest of the universe, but does not absorb or emit electromagnetic radiation (hence, it is "dark"). Today it is estimated that dark matter comprises 84.5% of all matter in the universe [ii].

The existence of dark matter is betrayed also by the phenomenon of strong gravitational lensing. Predicted by Einstein in 1936 [iii], and observed first in 1979 [iv], strong gravitational lensing occurs when a massive, concentrated object like a galaxy or galaxy cluster lies between us and a more distant luminous object. As light travels to us from the more distant object, the gravity of the intermediate or lensing object bends the light as it passes by (Figure 3). This lensing effect can magnify, distort and multiply the image of the more distant object. For example, the quasar HE0435-1223 appears in four different places around the edge of its lensing galaxy (Figure 4).

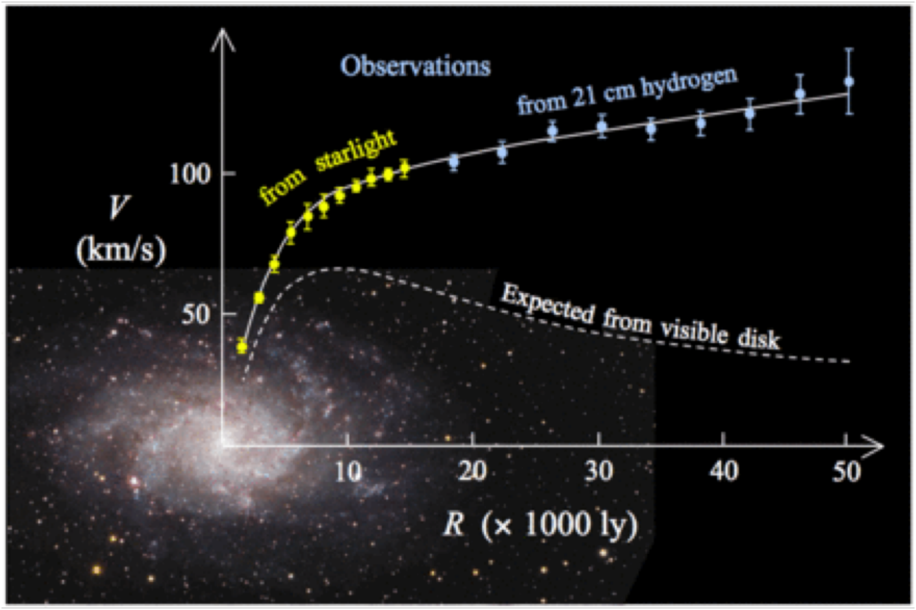

Figure 1: Observed and expected rotation curves of spiral galaxy M33. Wikipedia. The apparent mass distribution of the galaxy leads us to expect diminishing velocities with distance from the galactic center. But we observe increasing velocities. This suggests the presence of unseen mass, or dark matter, in the galaxy.

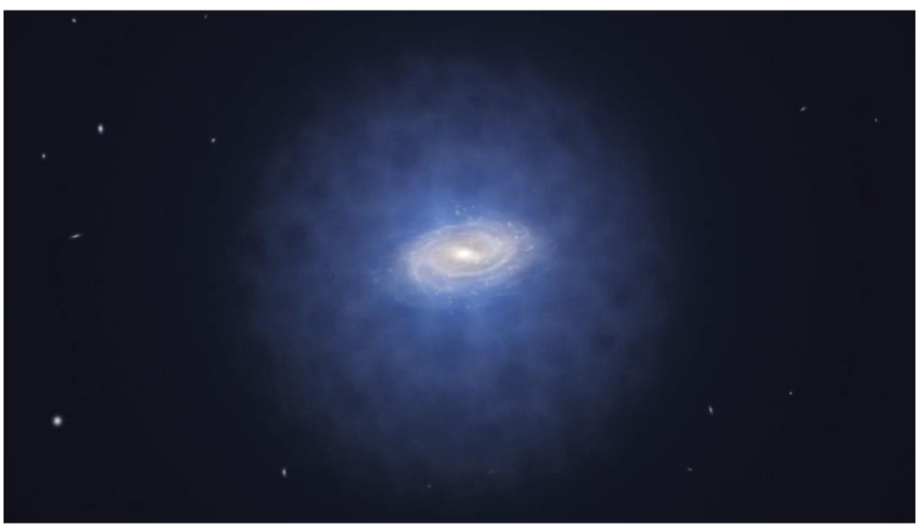

Figure 2: Artist's impression of the expected distribution of dark matter around the Milky Way galaxy. Image credit: European Southern Observatory (ESO)

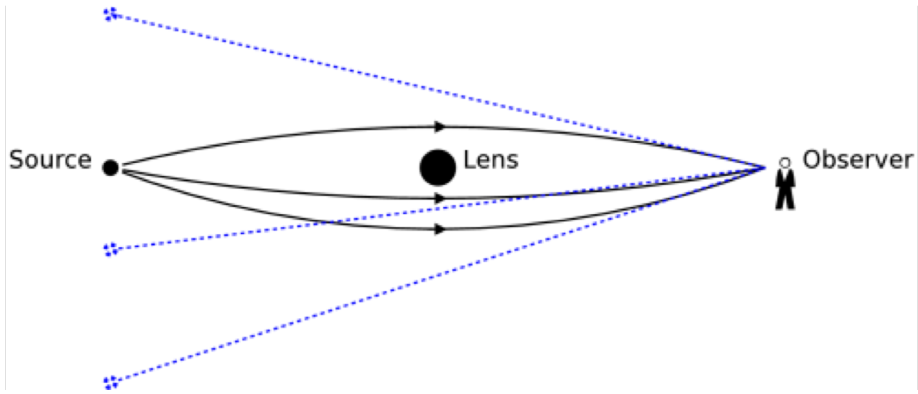

Figure 3: A diagram of strong gravitational lensing. Light is bent as it travels from a source (e.g. a distant quasar) through the strong gravitational field of a galaxy on its way to the observer. This bending of light creates multiple false images of the source (indicated in blue). Image source: http://en.citizendium.org/wiki/Gravitational_lens

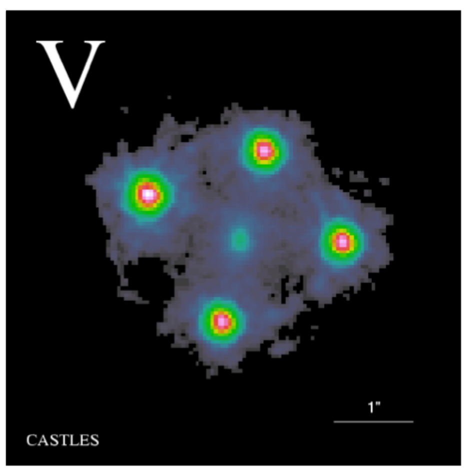

Figure 4: Hubble Space Telescope (HST) image of quadruply-imaged quasar HE0435-1223. Four images of the same quasar are created by gravitational lensing as light from the quasar is bent by the lensing galaxy in the center. Image source: https://www.cfa.harvard.edu/castles/Individual/HE0435.html

Gravitationally lensed quasars like HE0435-1223 can teach us about dark matter, because the distribution of dark matter in the lensing galaxy contributes to the lensing effect. Among other effects, lensing introduces a significant time delay (on the order of hours and days) between the images produced by lensing. This is due partly to the fact that light from each image has a different path length, and partly to the fact that the light travels through different parts of the lensing galaxy. These delays are noticeable when the brightness of the lensed object fluctuates significantly and quickly as quasars do. The same series of fluctuations observable in one image will be observable in the other images hours or days later. If the time delays between images can be measured precisely, they can tell us about the structure of dark matter in the lensing galaxy [v].

2 Pilot Project Objectives

Leonidas Moustakas (JPL/Caltech) is leading a pilot project to measure the time delays in two gravitationally lensed quasars, HE0435-1223 and RXJ1131-1231, using images from ground-based telescopes in the Las Cumbres Observatory Global Telescope network (Figure 5). The project aims to measure the time delays precisely enough to place constraints on the dark matter substructure of the lensing galaxy, which requires measuring the delays to a precision of ~ 1 hour with a reproducible photometric precision of a few percent. These are challenging objectives to meet due to the crowded field and the atmospheric distortion present in ground-based images (Figure 6).

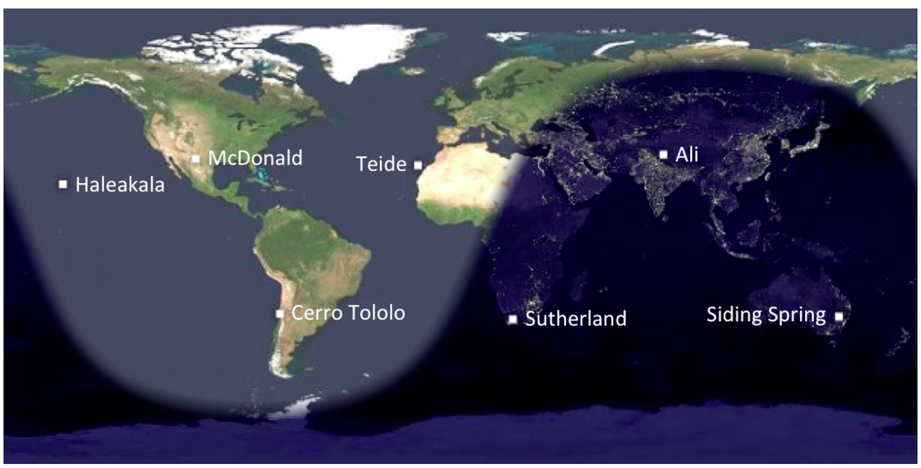

Figure 5: Las Cumbres Observatory Global Telescope network observatory sites. The three sites in the southern hemisphere (Cerro Tololo, Sutherland, and Siding Spring) provided about a day and a half of continuous observation of HE0435-1223, which produced over 400 five-minute exposures. Source: https://lcogt.net/observatory/sites/

3 Internship Objectives

In order to know whether the pilot project has attained the required precision in its measurements, we must have reliable estimates of the photometric uncertainties. In order to determine

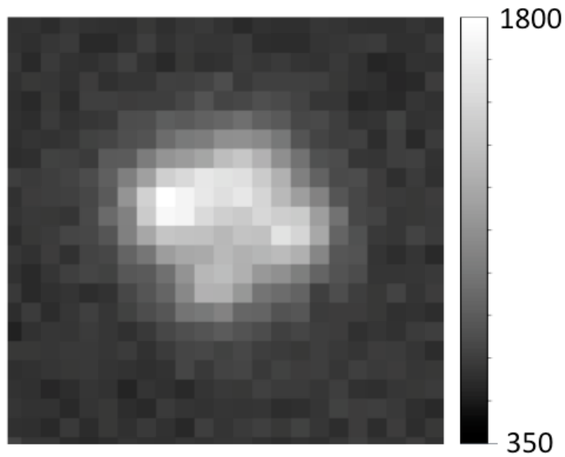

Figure 6: One of the ground-based images of HE0435-1223 from the Cerro Tololo site in the Las Cumbres Observatory Global Telescope network. The four quasar images are separated by ~ 2 arcsec. The frame is 20 pixels on a side, and the pixel scale is 0.387 arcsec/pixel. The color bar indicates total flux per pixel.

these uncertainties, the photometric methods used on the real data will be applied to a set of simulated astronomical images, indistinguishable from the real data, except that the simulated images will be produced with known time delays. The results of these measurements can then be compared with the known values in order to estimate the uncertainties in the measurements of the real time delays.

The primary objective of my internship is to develop the computer code that will produce the simulated images with known time delays.

4 Methods

The image simulator is coded in Python using the GalSim image simulation toolkit [vi]. Among other capabilities, GalSim provides a Python class library for generating images of astronomical objects such as stars and galaxies, and for performing image transformations and operations such as convolution.

The image simulator reads user-defined parameters from several data files. It reads general observational parameters, object parameters, and the fluctuating magnitudes of the quasar images, and produces a folder of simulated FITS files, a folder of PNG files, a FITS data cube containing all of the images in a single file, and an animated GIF of the simulated images. These inputs and outputs are illustrated in Figure 7.

The observational parameters are read from a plain text file (Figure 8), and include the size of the image [pixels], the location of the image center [RA DEC], the pixel scale [arcsec/pixel], the exposure time [s], and any other observational parameters that should be constant for all observations.

The object parameters are read from two CSV files. The parameters for reference objects with unchanging magnitude (e.g. reference stars) are read from one file. And the parameters for the objects with fluctuating magnitude (e.g. the quasar images) are read from another file. These objects are defined by 'profiles', which take several required and optional parameters.

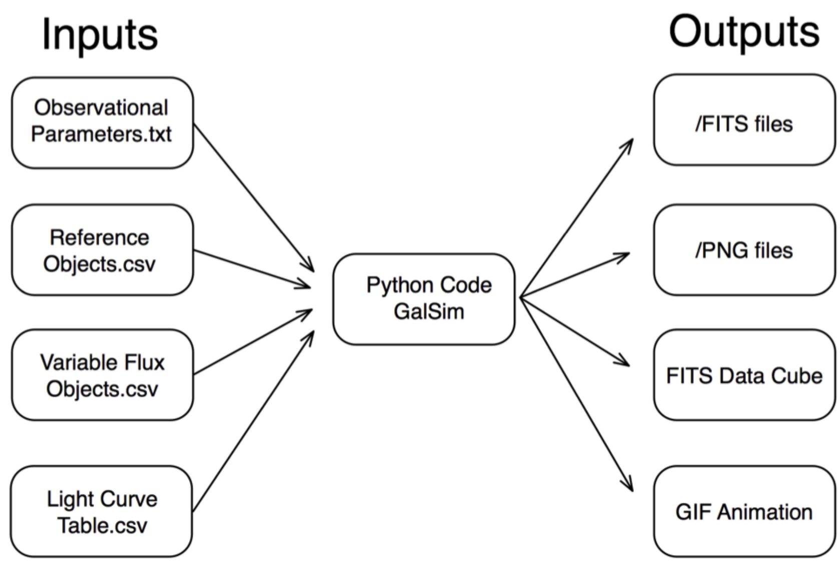

Figure 7: Flowchart of the inputs and outputs of the Python image simulation code.

The supported profiles and their parameters are displayed in Figure 9. For example, the Moffat profile requires a seeing parameter, beta, and either the full-width-at-half-maximum (FWHM) or the half-light radius.

Figure 10 shows a table of parameters for the four HE0435-1223 images. The images are labeled 'A', 'B', 'C', and 'D', and given positions in world coordinates. All the images are modeled with Moffat profiles, which require the seeing parameter, beta, and either the FWHM or the half-light radius. In this case, these are estimated very roughly to be 2.0 and 1.5. The images are also given ellipticity and position angle, although these are only dummy values until values can be obtained from analysis of the real images.

The fluctuating magnitudes of the quasar images are read from a simulated light curve table that is generated by previously developed code. The code generates random fluctuations in magnitude that are staggered between the quasar images by known time delays. The first few rows and columns of such a table are shown in Figure 11. The image simulation code reads the Modified Julian Dates and the magnitudes of the images from this table, and generates a FITS file for each date.

5 Results

The simulator produces images in the FITS file format, which is a standard format for digital astronomical images. A sample image is shown in Figure 12 next to a real image from the Cerro Tololo observatory for comparison. The simulated image is not an exact replica of the real image, because the parameters have been only roughly estimated or dummy values have been used. More finely tuned parameters will be obtained from more thorough analysis of the

```
instructions
------------

any line without an equals sign will be skipped over
put no spaces before or after the equals sign
comments begin with #
precede # with a single space

general observational parameters
--------------------------------

img_size=20 # pixels
img_center=04:38:14.9 -12:17:14.4 # RA DEC
pixel_scale=0.387 # arcsec/pixel
exp=300 # exposure time [s]

```

Figure 8: The text file containing the general observational parameters.

Profile	Par-1	Par-2	Par-3
Gaussian	Sigma	FWHM	Half Light Radius
	(one of these three is required)		
Moffat	Beta	FWHM	Half Light Radius
	(required)	(one of these two)	
Sersic	Sersic index	Half Light Radius	Truncation Radius
	(required)	(required)	(optional)
De Vaucouleurs	Half Light Radius	Truncation Radius	--
	(required)	(optional)	--

Figure 9: The supported object profiles and their required and optional parameters. For Sersic and de Vaucouleurs profiles, a truncation radius can be specified (in arcsec) to reduce computation time. Otherwise, GalSim computes the broad tails of the profiles to infinity.

<Table masked=True length=4>

object	RA	DEC	profile	par_1	par_2	par_3	e	PA
string8	string80	string88	string48	int64	float64	int64	float64	float64
A	4:38:14.90	-12:17:14.4	Moffat	2	1.5	--	0.19	174.8
B	4:38:14.80	-12:17:13.8	Moffat	2	1.5	--	0.19	174.8
C	4:38:14.74	-12:17:15.0	Moffat	2	1.5	--	0.19	174.8
D	4:38:14.84	-12:17:16.0	Moffat	2	1.5	--	0.19	174.8

Figure 10: Table of parameters for the four images of quasar HE0435-1223. All four images are modeled with Moffat profiles. The ellipticity, e, and position angle, PA, are dummy values.

<Table masked=False length=5>

mjd	A	A_err	B	B_err
float64	float64	float64	float64	float64
57008.0353569	18.8731703591	0.0530443106089	19.0879651634	0.060415
57008.0394209	18.7595799868	0.0453976896729	19.1258702467	0.054267
57008.0434403	18.6490061144	0.0395123072262	19.1269654999	0.049494
57008.0515023	18.7489634622	0.0394208564428	19.2689542318	0.051463
57008.0555272	18.6906241489	0.0376486130515	19.1746525582	0.047221

...

Figure 11: The first few rows and columns of a simulated light curve table with modified julian date, magnitudes and uncertainties for the four quasar images.

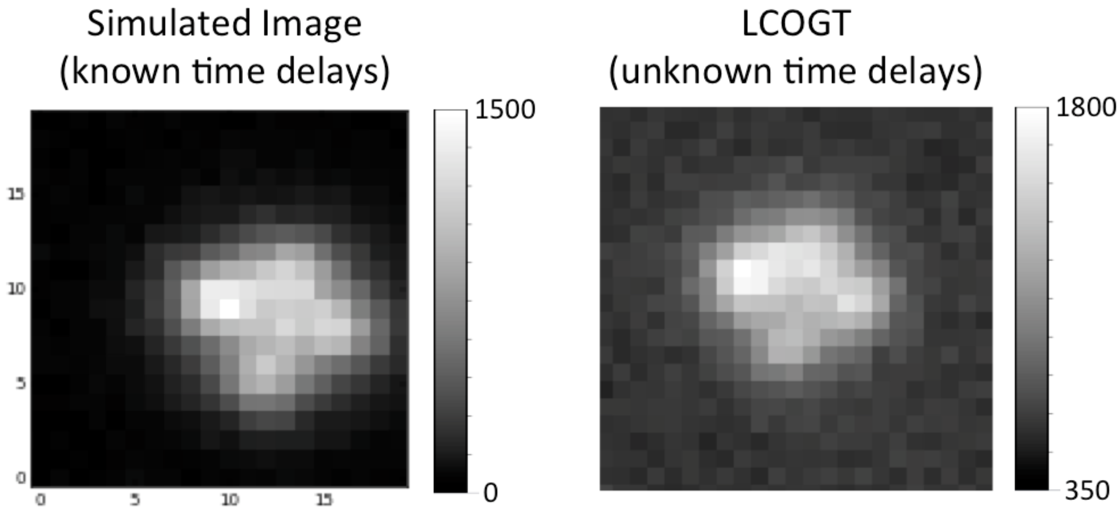

Figure 12: Left: Simulated image of HE0435-1223 with known time delays. Right: Real image of HE0435-1223 with unknown time delays. The color bars indicate total flux per pixel.

real images. For example, the correct object profile (Gaussian, Moffat, etc.), profile parameters, ellipticity and position angle, will be more accurately determined once the PSF-fitting of the real images is finished by other members of the team. Once the real images are fit well, those parameters can be entered into the simulation code to produce more accurate simulations.

In principle, the simulated images should be indistinguishable from the real images, except that they will have different (and known) time delays. Investigators can then apply their photometric methods to the simulated images just as they would to real images from telescopes. They can compare the results of their photometric analysis with the known time delays in the simulated images in order to determine the uncertainties in their measurements.

6 References

[i] Freeman, K.; McNamara, G. (2006). In Search of Dark Matter. Birkhuser. p. 37.

[ii] Francis, Matthew (22 March 2013). "First Planck results: the Universe is still weird and interesting". Arstechnica.

[iii] Einstein, A. Science 84 (1936), p. 506.

[iv] Walsh et al. Nature 279 (1979), 381 – 384.

[v] Moustakas, L. "Strong Gravitational Lensing by Galaxies". The Hellenic Astronomical Society Newsletter 2/7 (June 2010), 12 – 16.

[vi] Rowe et al. "GalSim: The modular galaxy image simulation toolkit". arXiv:1407.7676v3 [astro-ph.IM]. 30 Jul 2014.